A Theoretical Study of Stereochemistry of 1,3-Migration in Allylsilane and Related Allylmetallic Compounds

Masae Takahashi[†] and Mitsuo Kira*[,†,‡]

Contribution from the Photodynamics Research Center, The Institute of Physical and Chemical Research (RIKEN), 19-1399, Koeji, Nagamachi, Aoba-ku, Sendai 980, Japan, and Department of Chemistry, Graduate School of Science, Tohoku University, Aoba-ku, Sendai 980-77, Japan

Received August 29, 1996. Revised Manuscript Received December 13, 1996[⊗]

Abstract: Ab initio MO calculations for the concerted 1,3-silyl migration in allylsilane at Hartree−Fock and multiconfigurational levels revealed the existence of two transition structures (TS), which lead to retention and inversion of stereochemistry at the silicon. The two structures are pentacoordinate square pyramidal and trigonal bipyramidal around the silicon atom, respectively. The energy barriers estimated at various levels of calculation, including those with electron correlation effects, indicate that the retention transition structure is ca. 9 kcal/mol more stable than the inversion transition structure, in contrast to the experimental results of Kwart et al. Introduction of a π system, such as a vinyl group, at the silicon stabilizes the inversion TS more than the retention TS. Similar transition structures and energetics were obtained for 1,3-migration in allylgermane and allylstannane using effective core potentials for Ge and Sn.

Introduction

Among the very large number of facile 1,3-silyl migrations known to date, the migration of a silyl group from carbon to carbon is of particular interest from a mechanistic viewpoint.[1] Whereas 1,3-silyl migration in β-keto silanes, a typical 1,3-silyl migration from carbon to heteroatom, is considered as an intramolecular nucleophilic substitution and actually proceeds with retention of configuration at silicon,[2] the thermal 1,3-silyl migration in allylic silanes has been shown by Kwart et al. to proceed concertedly with inversion of configuration at the migrating silicon;[3] the activation enthalpy (ca. 48 kcal/mol) is considerably lower than the Si−C dissociation energy. Following the Woodward−Hoffmann rules,[4] Kwart et al. have proposed the orbital diagram for the migration as shown in Scheme 1. Their mechanism assumes implicitly the rather unusual trigonal bipyramidal (TBP) transition structure at the pentacoordinate silicon, where the two axial positions are occupied by allylic carbons. Alternatively, the migration may proceed with retention of configuration at the silicon by taking a square pyramid (SP) structure around the silicon (Scheme 2).

We have investigated in detail the transition structures (TS) and the stereochemistry of 1,3-silyl migration in allylsilane and the related migration in 1-butene, allylgermane, and allylstannane by using ab initio molecular orbital theory.

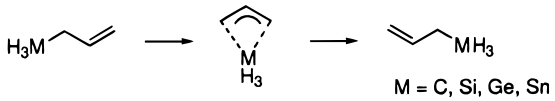

TS

Two transition structures with a retention (TS_{ret}) and an inversion (TS_{inv}) configuration were optimized for 1,3-silyl migration in allylsilane at HF/6-31G*, MP2/6-31G*, and DFT/6-31G* levels. The TS_{inv} is a distorted TBP around the silicon *with the two allylic carbons at the equatorial positions*, different from the TS illustrated by Kwart et al., while the TS_{ret} is a distorted SP structure around silicon. Rather unexpectedly, the TS_{ret} is more stable than the TS_{inv} at all levels of calculations performed, in contrast to the experimental results by Kwart et al. Calculations of the effects of substituents at silicon on the geometry and energy of the transition structures suggest that both electronic and steric effects may account for the discrepancy between theory and experiment. Similar features were obtained for the transition structures and energetics of 1,3-migrations in allylgermane and allylstannane, calculated using effective core potentials for Ge and Sn.

Scheme 1

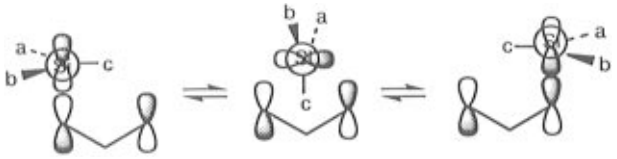

Scheme 2

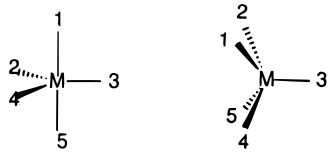

Methods

Computational Details. Calculations at Hartree−Fock (HF) and multiconfigurational (MCSCF) levels were performed by using the

* Author to whom correspondence should be addressed.
† RIKEN.
‡ Tohoku University.
⊗ Abstract published in *Advance ACS Abstracts,* February 1, 1997.

(1) For a review, see: Brook, A. G.; Bassindale, A. R. *Rearrangements in Ground and Excited States*; de Mayo, P., Ed.; Academic Press: London, 1980; Vol. 2, Essay 9.
(2) Brook, A. G.; MacRae, D. M.; Limburg, W. W. *J. Am. Chem. Soc.* **1967**, *89*, 5493.
(3) (a) Kwart, H.; Slutsky, J. *J. Am. Chem. Soc.* **1972**, *94*, 2515. (b) Slutsky, J.; Kwart, H. *J. Am. Chem. Soc.* **1973**, *95*, 8678.
(4) Woodward, R. B.; Hoffmann, R. *The Conservation of Orbital Symmetry*; Academic Press: New York, NY, 1970.

S0002-7863(96)03050-8 CCC: $14.00

Gaussian 90, Gaussian 92, and Gaussian 94 computer programs.[5] Standard 6-31G* basis sets were used for all geometry optimization and pathway studies. In addition, to check the effects of additional polarization functions and diffusion functions, some of selected structures were optimized at 6-31G, 6-31G**, and 6-31+G* levels. The adequacy of the single-reference calculations was tested by performing the CISD/6-31G* calculations on ground state and transition structures of allylsilane. The analysis of the configuration interaction (CI) wave function indicated that the single HF reference provided an appropriate description; only a doubly excited configuration had a coefficient larger than 0.03 (0.04) apart from the HF reference.[6] The Hay and Wadt effective core potential was used for calculations of allylgermane and allylstannane at double-ζ basis sets (Lanl1DZ).[7] Transition structures were found by the eigenvector-following method. Some optimizations were carried out with MP2(fc) and density functional theory (DFT) methods. To study the effects of electron correlation, single-point energies were obtained using the MP2(fc), CCSD, CISD, and MCSCF methods on the HF/6-31G*-optimized geometry. The MCSCF calculations were of the complete-active-space (CASSCF) type with four electrons in four orbitals (i.e., the orbitals which are composed mainly of three carbon 2p orbitals and one silicon 3p orbital). The calculations using density functional theory (DFT) were performed with the nonlocal exchange potential of Becke[8] together with the nonlocal correlation function of Perdew.[9]

Assessment of Distortion in Transition Structures from Ideal Pentacoordinated Structures. Holmes et al. have shown that the structure around a pentacoordinate atom is described as an intermediate between the idealized TBP and SP.[10] The displacement of the calculated transition structures from TBP to SP was therefore estimated in percentage according to the method of Holmes et al. The numbering schemes in TBP and SP used in the calculations are shown in Scheme 2. Thus, ligands 1 and 5 were selected so that θ_{15} is the largest bond angle among ten θ_{ij} values, representing angles i−M−j. Dihedral angles were measured with unit bond distance. The dihedral angle δ_{24}, which is defined as the angle between normals of the two planes 1−2−4 and 5−2−4, was selected to be the smallest dihedral angle among nine dihedral angles.

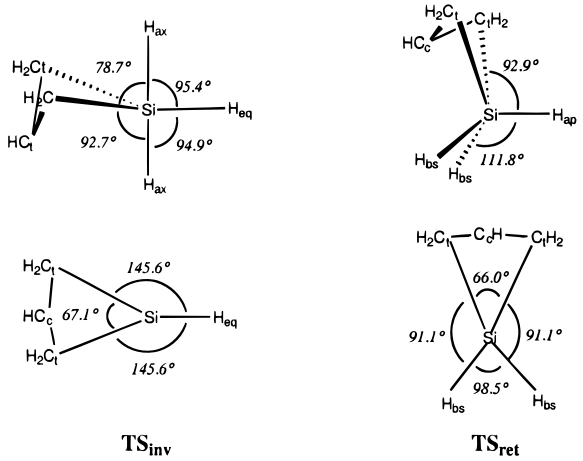

TS$_{inv}$ **TS$_{ret}$**

Figure 1. Optimized transition structures for 1,3-silyl migrations with inversion (TS$_{inv}$) and retention (TS$_{ret}$) of configuration at silicon using HF/6-31G* calculations. The lower part shows the equatorial plane of TS$_{inv}$ and the basal plane of TS$_{ret}$. Selected bond distances (Å) for TS$_{inv}$: C$_t$−Si, 2.262; C$_c$−Si, 2.252; C$_t$−C$_c$, 1.398. Selected bond distances (Å) for TS$_{ret}$: C$_t$−Si, 2.264; C$_c$−Si, 2.149; C$_t$−C$_c$, 1.394.

Results and Discussion

Geometry of CH_2=$CHCH_2MH_3$ (M = C, Si, Ge, and Sn). The structure and torsional potential function of allylsilane have been investigated by Cartledge et al. using the 3-21G* basis set.[11a] Whereas our 6-31G* level calculations give slightly better agreement with the experimental values[11b−d] than the previous calculations at 3-21G* level, the structural features are essentially the same.[12] At the optimized structure, the dihedral angle δ(CCCM) of 1-butene is indicative of the typical gauche structure (120°) in the most preferred conformation, while the corresponding dihedral angles for allylsilane, allylgermane, and allylstannane are significantly smaller than that for 1-butene and are in the order Si (109°) > Ge (108°) > Sn (105°) (at Lanl1DZ level) due to the enhanced hyperconjugation which becomes more important in the inverse order.

Transition Structures. Two transition structures with C_s symmetry were optimized at RHF/6-31G* level for suprafacial 1,3-silyl migration in allylsilane. One is the transition structure with retention of configuration (TS$_{ret}$) and the other is that with inversion of configuration (TS$_{inv}$) at the migrating silicon. The selected structural parameters are given in Figure 1.[12] Each transition structure has one imaginary frequency with the vibrational mode directing toward the 1,3-silyl migration. Intrinsic reaction coordinate (IRC) calculations have confirmed that these transition structures are responsible for the 1,3-silyl migration. Symmetry-broken UHF calculations at the 6-31G* level gave the identical transition structures and energies to those obtained by RHF calculations. Thus, the 1,3-silyl migration is classified as a closed-shell reaction throughout the entire reaction pathway.

The optimized transition structures for the 1,3-silyl migration depend a little on the basis sets and the levels. The structures found at 6-31G** and 6-31+G* levels are essentially identical to the 6-31G* structure, while the C−Si distances at the 6-31G level are longer by 0.1−0.2 Å than those at the 6-31G* level. Introduction of polarization functions gives rise to shrinkage of the four-membered ring made of silicon and allyl carbons.

(5) (a) Frisch, M. J.; Head-Gordon, M.; Trucks, G. W.; Foresman, J. B.; Schlegel, H. B.; Raghavachari, K.; Robb, M.; Binkley, J. S.; Gonzalez, C.; Defrees, D. J.; Fox, D. J.; Whiteside, R. A.; Seeger, R. A.; Melius, C. F.; Baker, J.; Martin, R. L.; Kahn, L. R.; Stewart, J. J. P.; Topiol, S.; Pople, J. A. *Gaussian 90*; Gaussian, Inc.: Pittsburgh, PA, 1990. (b) Frisch, M. J.; Trucks, G. W.; Head-Gordon, M.; Gill, P. M. W.; Wong, M. W.; Foresman, J. B.; Johnson, B. G.; Schlegel, H. B.; Robb, M. A.; Replogle, E. S.; Gomperts, R.; Andres, J. L.; Raghavachari, K.; Binkley, J. S.; Gonzalez, C.; Martin, R. L.; Fox, D. J.; Defrees, D. J.; Baker, J.; Stewart, J. J. P.; Pople, J. A. *Gaussian 92*; Gaussian, Inc.: Pittsburgh, PA, 1992. (c) Frisch, M. J.; Trucks, G. W.; Schlegel, H. B.; Gill, P. M. W.; Johnson, B. G.; Robb, M. A.; Cheeseman, J. R.; Keith, T. A.; Petersson, G. A.; Montgomery, J. A.; Raghavachari, K.; Al-Laham, M. A.; Zakrzewski, V. G.; Ortiz, J. V.; Foresman, J. B.; Cioslowski, J.; Stefanov, B. B.; Nanayakkara, A.; Challacombe, M.; Peng, C. Y.; Ayala, P. Y.; Chen, W.; Wong, M. W.; Andres, J. L.; Replogle, E. S.; Gomperts, R.; Martin, R. L.; Fox, D. J.; Binkley, J. S.; Defrees, D. J.; Baker, J.; Stewart, J. P.; Head-Gordon, M.; Gonzalez, C.; Pople, J. A. *Gaussian 94*; Gaussian, Inc.: Pittsburgh, PA, 1995.

(6) (a) Nyulászi, L.; Szieberth, D.; Veszprémi, T. *J. Org. Chem.* **1995**, *60*, 1647. (b) A similar analysis of the CI wave function for 1,3-methyl migration of 1-butene shows relatively large contribution from the HOMO−LUMO doubly excited configuration (the coefficient of 0.14 for both transition states with retention and inversion of configuration), while the contribution from singly excited configurations is negligibly small (the coefficient of 0.04 only for the transition state with inversion which has extremely higher activation barrier than the other transition states calculated in this paper). Thus, transition structures for the 1,3-methyl migration can be considered as well-describable by a single determinant wave function.

(7) (a) Hay, P. J.; Wadt, W. R. *J. Chem. Phys.* **1985**, *82*, 270. (b) Wadt, W. R.; Hay, P. J. *J. Chem. Phys.* **1985**, *82*, 284. (c) Hay, P. J.; Wadt, W. R. *J. Chem. Phys.* **1985**, *82*, 299.

(8) Becke, A. D. *Phys. Rev.* **1988**, *A38*, 3098.

(9) Perdew, J. P. *Phys. Rev.* **1986**, *B33*, 8822.

(10) (a) Holmes, R. R.; Deiters, J. A. *J. Am. Chem. Soc.* **1977**, *99*, 3318. (b) Holmes, R. R.; Day, R. O.; Harland, J. J.; Sau, A. C.; Holmes, J. M. *Organometallics* **1984**, *3*, 341.

(11) (a) Profeta, S., Jr.; Unwalla, R. J.; Cartledge, F. K. *J. Org. Chem.* **1986**, *51*, 1884. (b) Frierson, M. R. Ph.D. Dissertation, University of Georgia, 1984. (c) Beagley, B.; Foord, A.; Montran, R.; Rozsondai, B. *J. Mol. Struct.* **1977**, *42*, 117. (d) Hayashi, M.; Imachi, M.; Saito, M. *Chem. Lett.* **1977**, 221.

(12) Detailed geometrical parameters are given in Supporting Information.

Transition structures optimized using MP2/6-31G* and DFT/6-31G* levels are very close to the HF/6-31G* structure.

To classify these transition structures from the viewpoint of pentacoordinate silicon chemistry, the deviation from idealized TBP structure (%SP) was estimated for TS_{ret} and TS_{inv} at the HF/6-31G* level according to Holmes et al.[10] The values of %SP of TS_{ret} and TS_{inv} are 88.8 and 14.5%, respectively. Thus, the TS_{ret} has a SP structure displaced 11% toward TBP, while TS_{inv} has a TBP structure displaced 15% toward SP. In the TS_{ret}, one silyl hydrogen (H_{ap}) occupies the apical position of the SP structure and the other four ligands are at the basal positions. It should be noted that the TBP structure is different from that assumed by Kwart et al.[3] In the calculated TS_{inv}, two silyl hydrogens (H_{ax}) occupy the axial position of TBP and the other silyl hydrogen (H_{eq}) and two allylic terminal carbons (C_t) make an equatorial plane, whereas in the TS of Kwart et al. two terminal carbons occupy the axial positions and three silyl hydrogens make an aquatorial plane. Summation of the three bond angles, C_t-Si-C_t and two C_t-Si-H_{eq}, of TS_{inv} gives 358.3°, which indicates that the silicon atom is located essentially in the equatorial plane; the angle of $H_{ax}-Si-H_{ax}$ in the TS_{inv} is 169.7°, which is close to the 180° angle of the ideal TBP structure.

Similarly, two transition structures were found for 1,3-migrations in allylgermane, allylstannane, and 1-butene.[12] For calculations of germyl and stannyl migrations, Hay and Wadt effective core potential is used at double-ζ basis set.[7]

In all TS_{inv} species, distances between the central atom (M) and the allylic central carbon (C_c) and between M and the allylic terminal carbon (C_t) are similar (the difference between the C_c-M and C_t-M distances is 0.009−0.056 Å depending on M and basis set); the angles of $M-C_c-C_t$ and $M-C_c-H$ are 72−75° and 109−115°, respectively. On the other hand, in TS_{ret}, the C_c-M distance is distinctly shorter than the C_t-M distance (the difference between the C_c-M and C_t-M distances is 0.064−0.612 Å depending on M and basis set). It is suggested that there is significant contribution of the subjacent orbital control for the stabilization of TS_{ret} (*vide infra*). The TS_{ret} and TS_{inv} for allylgermane and allylstannane are also ascribed to partially distorted SP and TBP structures, respectively. In the TS_{ret} and TS_{inv} for 1,3-methyl migration, the elongation of the $C_t-M(C)$ bond amounts to more than 50% of the normal C−C single bond, and therefore, the assignment to the pentacoordinate geometry is no longer substantial.

Bernardi et al. have reported that there is a transition state for a 1,2-methyl migration in 1-butene.[13] We have therefore investigated a possible 1,2-migration in allylsilane, which may compete with 1,3-migrations. Actually, a transition structure for the 1,2-silyl migration (TS_{12}) in allylsilane was found at the UHF/6-31G* level; the TS_{12} leads to an open-shell biradical intermediate. Whereas the configuration at silicon of the optimized TS_{12} is retention, the structure is ultimately different from TS_{ret}; the two C_t-Si distances in TS_{12} are different from each other (2.240 and 2.809 Å), while they are the same in the TS_{ret} (2.264 Å). The structure and energy of TS_{12} are very close to those of the biradical intermediate.

Activation Energy. First, the basis set and level dependence on the activation energies (E_a values) for 1,3-silyl migration in allylsilane are compared. The results are summarized in Table 1. Increasing the polarization functions or adding extra diffusion functions to the 6-31G* basis set exerts no significant effects on the E_a values, while the basis set without polarization functions (6-31G) increases the E_a values for both TS_{ret} and TS_{inv}. The energy difference (ΔE_a) between the two transition states is much smaller at the 6-31G level compared with those at the higher level of calculations; the inclusion of the polarization functions is essential to obtain reliable E_a values. Optimization by DFT and MP2 methods at the 6-31G* level gives slightly lower E_a values than the corresponding simple HF calculations.

Table 1. Activation Energies (E_a) for 1,3-Silyl Migrations with Inversion (TS_{inv}) and Retention (TS_{ret}) and the Energy Difference (ΔE_a) at Various Levels of Calculation[a]

level	E_a		ΔE_a[b]
	TS_{ret}	TS_{inv}	
HF/6-31G	73.6	79.4	5.8
HF/6-31G*	64.0	75.1	11.1
HF/6-31G**	63.9	75.2	11.3
HF/6-31G*	64.6	76.1	11.5
MP2/6-31G*	52.8	62.7	9.9
DFT/6-31G*	44.8	53.1	8.3

[a] Geometry was fully optimized at the indicated level. The energy is given in kcal/mol. [b] $\Delta E_a = E_a(\text{inv}) - E_a(\text{ret})$.

Table 2. Activation Energies for 1,3-Silyl and 1,2-Silyl Migrations, the Energy Difference between Inversion and Retention Transition States (ΔE_a), and Bond Dissociation Energy (BDE) Obtained by Single-Point Calculations at the HF/6-31G* Optimized Geometry.[a]

level	E_a			ΔE_a[d]	BDE[e]
	TS_{ret}[b]	TS_{inv}[b]	TS_{12}[c]		
HF/6-31G*	64.0	75.1	57.6	11.1	46.3
MP2/6-31G*	53.9	62.8	67.7	8.9	78.6
MP4SDQ/6-31G*	57.2	66.4	66.0	9.2	72.8
MP4SDTQ/6-31G*	51.3	60.0	62.7	8.7	75.5
QCISDT/6-31G*	55.7	64.3	58.2	8.6	70.2
ST4CCD/6-31G*	56.1	64.6	65.8	8.5	73.6
HF/6-31+G(3df,2p)	61.6	74.4	56.7	12.8	45.8
MP2/6-31+G(3df,2p)	48.4	57.9	64.7	9.6	83.1
MCSCF/6-31G*	64.0	75.1		11.1	
MP2-MCSCF/6-31G*	54.2	59.8		5.6	

[a] Given in kcal/mol. [b] Calculated using RHF wave functions. [c] Calculated using UHF wave functions. [d] $\Delta E_a = E_a(\text{inv}) - E_a(\text{ret})$. [e] Bond dissociation energy is calculated as the energy difference between the total energy of allylsilane and the sum of the total energies of allyl and silyl radicals optimized at UHF/6-31G*.

In Table 2, the E_a values of TS_{ret} and TS_{inv} for 1,3-silyl migration and the ΔE_a are compared at various levels of single-point calculations at the HF/6-31G*-optimized geometry. All of the single-point calculations at various levels of perturbation theories of Moller−Plesset (MP2, MP3, MP4D, MP4DQ, MP4SDQ, MP4SDTQ), configuration interactions (QCISD, QCISDT), and coupled cluster (CCD, ST4CCD) give similar results for the E_a values of TS_{ret} (51.3−58.3 kcal/mol) and TS_{inv} (60.0−67.2 kcal/mol) as well as ΔE_a (8.5−9.2 kcal/mol). Single-point calculations using a much larger basis set (HF/6-31+G(3df,2p)) confirm that the larger set of polarization gives no serious effects on the E_a values and ΔE_a; ΔE_a values at the HF/6-31+G(3df,2p) basis set are only slightly larger than those at the 6-31G* basis set (the ΔE_a differences are 1.7 and 0.7 kcal/mol at the HF and MP2 levels, respectively). In contrast to the experimental results by Kwart et al.,[3] the various calculations suggest that the retention pathway is preferred to the inversion pathway for 1,3-silyl migration in allylsilane.

As another mechanism for 1,3-silyl migration in allylsilane, a dissociation−recombination sequence of the allylic carbon−silicon bond should be considered. The bond dissociation energy (BDE) of the silicon−carbon bond was calculated using unrestricted open-shell wave functions for allyl and silyl radicals, and the values are included in Table 2. The BDE values of the

(13) Bernardi, F.; Olivucci, M.; Robb, M. A.; Tonachini, G. *J. Am. Chem. Soc.* **1992**, *114*, 5805.

Table 3. Comparison of Activation Energies for 1,3-Migrations in $CH_2{=}CHCH_2MH_3$ (M = C, Si, Ge, and Sn)[a]

	C	Si		Ge	Sn
	6-31G*	6-31G*	Lanl1DZ	Lanl1DZ	Lanl1DZ
E_a(ret)	133.6	64.0	79.6	72.9	55.4
E_a(inv)	116.9	75.1	84.6	77.5	62.3
ΔE_a[b]	−17.7	11.1	5.0	4.6	6.7

[a] Geometry was fully optimized at the indicated level. The energy is given in kcal/mol. [b] $\Delta E_a = E_a(\text{inv}) - E_a(\text{ret})$.

MP2 calculation are in good accord with the expected BDE,[14] indicating that the incorporation of the electron correlation effects is necessary for the calculation of BDE, as pointed out by Boyd et al.[15] Basis set superposition errors (BSSE) for BDE of allylsilane are evaluated to be only 2 kcal/mol by performing counterpoise calculations at the RHF/6-31G* level.[16] Since the BDE for the silicon−carbon bond is much higher than the activation energies for both TS_{ret} and TS_{inv}, the dissociation−recombination mechanism would not compete with the two concerted pathways.[17]

Activation energies for various 1,3-migrations optimized at the HF/6-31G* and Lanl1DZ are summarized in Table 3. The E_a values for both TS_{ret} and TS_{inv} in allylmetallic compounds (M = Si, Ge, and Sn) decrease in the order of Si > Ge > Sn at the same Lanl1DZ level. The ΔE_a values for the migration in allylgermane and allylstannane are comparable to the corresponding value for allylsilane; the 1,3-migration with retention is favored over that with inversion. However, since the E_a values for allylgermane and allylstannane are higher than the BDE of Ge−C and Sn−C bonds,[14] concerted 1,3-migrations in these allylic metals may compete with the dissociation between the bonds.

For the 1,3-methyl migration in 1-butene, the E_a value for TS_{inv} is lower than that for TS_{ret}, which means that the Woodward−Hoffmann-allowed inversion pathway is preferred over the retention pathway. However, since the E_a values for the 1,3-methyl migration in 1-butene are much higher than the C−C bond dissociation energy,[14] the concerted 1,3-migration would not be able to compete with the homolytic C−C fission. There are a number of experimental and theoretical studies of the concerted [1,3]-sigmatropic migrations in rather sophisticated systems reported.[18−20]

Orbital Interactions in Transition States. We wish herein to analyze the molecular orbitals more in detail. The HOMOs for TS_{ret} and TS_{inv} are shown schematically in Figure 2. The HOMOs for the two transition structures are quite different from each other. Thus, the HOMO for TS_{inv} is comprised of the antisymmetric allyl π orbital (ϕ_2) and a 3pπ orbital on silicon, as predicted by the Woodward−Hoffmann rules. On the other hand, the HOMO for TS_{ret} is composed of ϕ_2 and a pseudo π orbital of two Si−H orbitals without significant contribution from a 3pπ orbital on silicon.

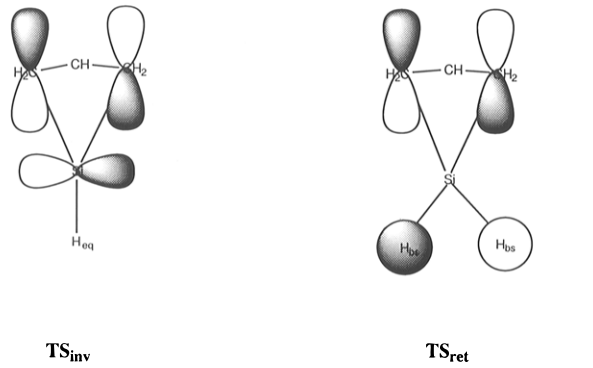

TS_{inv} **TS_{ret}**

Figure 2. Schematic representation of the HOMOs of TS_{ret} and TS_{inv} for 1,3-silyl migration in allylsilane.

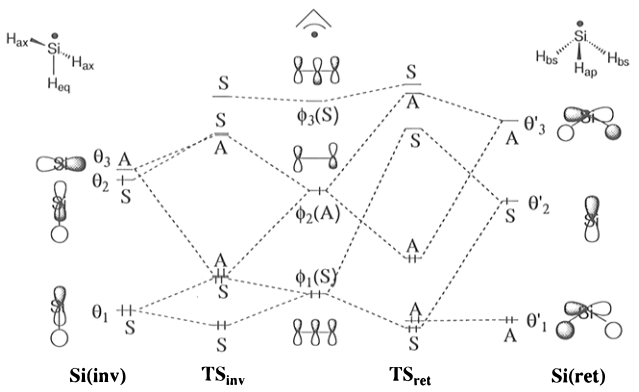

Figure 3. Orbital interaction diagram for the frontier orbitals of TS_{ret} and TS_{inv} for 1,3-silyl migration in allylsilane. The frontier orbitals are constructed by interaction among three π orbitals (ϕ_1, ϕ_2, and ϕ_3) of the allyl radical and three frontier orbitals (θ_1, θ_2, and θ_3) of the silyl radicals. The symmetry notations *S* and *A* refer to the plane bisecting allyl CCC plane.

The orbital sequences in the transition states are analyzed by using the orbital interaction diagram shown in Figure 3. The frontier orbitals in the transition structures are constructed by interaction among three π orbitals (ϕ_1, ϕ_2, and ϕ_3) of allyl radical and three frontier orbitals (θ_1, θ_2, and θ_3) of silyl radicals. Since the geometry of the silyl moiety is different in the two transition structures, the orbitals are calculated for the two different structures of silyl radicals, Si(ret) and Si(inv), at ROHF/6-31G* level; these structures are the same as those of the silyl moieties in the TS_{ret} and TS_{inv}, respectively. The frontier orbital sequences in TS_{ret} and TS_{inv} are quite well reconstructed by the orbital interaction between allyl radical π system and imaginary silyl radical frontier orbitals. The symmetry notations *S* and *A* refer to the plane bisecting the allyl CCC plane. Although in the TS_{inv} the MO interaction between the low-lying LUMO (θ_3) and the SOMO of allyl ϕ_2 orbital lowers the energy significantly as predicted by the Woodward−Hoffmann rules, the major stabilization in TS_{ret} is caused by the MO interaction between ϕ_1 and θ'_2 in addition to the interaction between ϕ_2 and θ'_3. As shown in a previous section, the C_c−Si distance in the TS_{ret} is significantly shorter than the C_t−Si distance; although the structure around silicon has been designated as pentacoordinated SP, the silicon may be regarded more accurately as hexacoordinated. When Si and C_c are brought into closer proximity, the MO interaction between ϕ_1 and θ'_2 will be strengthened. The reason for the lower E_a of TS_{ret} may be ascribed to the importance of this interaction, which should be regarded as a

(14) The BDE values of C−M in MMe_4 are reported to be 85.6, 74.4, 59.5, and 51.9 kcal/mol for M = C, Si, Ge, and Sn, respectively (*Comprehensive Organometallic Chemistry*; Wilkinson, G., Stone, F. G. A., Abel, E. W., Eds.; Pergamon Press: Oxford, 1982; Vol. 1, p 5.

(15) Boyd, S. L.; Boyd, R. J.; Barclay, L. R. C. *J. Am. Chem. Soc.* **1990**, *112*, 5724.

(16) Boys, S. F.; Bernaldi, F. *Mol. Phys.* **1970**, *19*, 553.

(17) Boyd, S. L.; Boyd, R. J.; Shi, Z.; Barclay, L. R. C.; Porter, N. A. *J. Am. Chem. Soc.* **1993**, *115*, 687.

(18) (a) Berson, J. A.; Nelson, G. L. *J. Am. Chem. Soc.* **1967**, *89*, 5503. (b) Berson, J. A.; Nelson, G. L. *J. Am. Chem. Soc.* **1970**, *92*, 1096. (c) Berson, J. A.; Salem, L. *J. Am. Chem. Soc.* **1972**, *94*, 8917. (d) Berson, J. A. *Acc. Chem. Res.* **1972**, *5*, 406.

(19) (a) Baldwin, J. E.; Belfield, K. D. *J. Am. Chem. Soc.* **1988**, *110*, 296. (b) Klarner, F.-G.; Drewes, R.; Hasselmann, D. *J. Am. Chem. Soc.* **1988**, *110*, 297.

(20) (a) Newman-Evans, R. H.; Carpenter, B. K. *J. Am. Chem. Soc.* **1984**, *106*, 7994. (b) Newman-Evans, R. H.; Simon, R. J.; Carpenter, B. K. *J. Org. Chem.* **1990**, *55*, 695. (c) Carpenter, B. K. *J. Am. Chem. Soc.* **1995**, *117*, 6336.

Table 4. Substituent Effects on the Structure and Energy for 1,3-Silyl Migration Calculated at the HF/6-31G* Level[a]

configuration	SiX_3	structure	substituent position	%SP[b]	E_a[c]	δE_a[c,d]
inversion	SiH_3	TBP		14.5	75.1	0
	SiH_2F	TBP	equatorial	13.9	64.3	−10.8
		TBP	axial	15.0	71.8	−3.3
		TBP	axial	15.4	76.4	1.3
	$SiHF_2$	TBP	axial, equatorial	15.2	70.7	−4.4
	SiH_2Me	TBP	equatorial	12.5	75.7	0.6
		TBP	axial	14.1	80.5	5.4
		TBP	axial	13.0	82.6	7.5
	$SiH_2(CH{=}CH_2)$	TBP	equatorial		71.1	−4.0
retention	SiH_3	SP		88.8	64.0	0
	SiH_2F	TBP[e]	axial	53.8	54.3	−9.7
	$SiHF_2$	TBP[e]	axial, equatorial	42.8	59.9	−4.1
		SP	basal	88.8	55.4	−8.6
	SiF_3	SP	two basal, one apical	50.4	61.3	−2.7
	SiH_2Me	SP	basal	85.7	64.0	0
		SP	apical	79.9	65.8	1.8
	$SiH_2(CH{=}CH_2)$	SP	apical		64.3	0.3

[a] Geometry was full optimized. [b] %SP is calculated by the method of Holmes et al.[10] See the Methods section. [c] Given in kcal/mol. [d] δE_a is defined as the substituent effects on the activation energy for the inversion or the retension pathway: $\delta E_a = E_a(SiX_3) - E_a(SiH_3)$. [e] In this TBP structure, two allyl carbons occupy the axial and equatorial positions.

type of subjacent orbital control, suggested by Berson for the 1,3-carbon migration.[18c,d]

Substituent Effects. As discussed above, the present theoretical study has shown that the retention pathway is preferred to the inversion pathway for 1,3-silyl migration in allylsilane. In order to elucidate the origin of the discrepancy between theoretical and experimental results, we investigated the substituent effects on the activation energy for 1,3-silyl migration in allylsilane in detail. Fluorine and the methyl group were selected as representatives of electron-withdrawing and -donating substituents, respectively. As initial structures for the search for the transition structures, one of the three hydrogens were simply replaced by substituents; three structures for TS_{inv} and two structures for TS_{ret} were considered. The results at the HF/6-31G* level are shown in Table 4.

Substitution of a fluorine atom at the equatorial position for TS_{inv} shows the largest stabilization and the smallest %SP. However, the fluorine substituent stabilizes the TS_{ret} equally and the ΔE_a (10.0 kcal/mol) is not influenced by the substitution. Substitution of two fluorine atoms for the TS_{inv} gives only one inversion transition structure. From an initial TS_{ret} (SP geometry) substituted by two fluorine atoms at the apical and a basal position, a highly distorted TBP transition state (%SP = 43) is obtained, where the two fluorine atoms occupy the axial and equatorial positions and two allylic carbons the other axial and equatorial positions. The largest stabilization is found when the two fluorine atoms are substituted at the basal positions of the TS_{ret}. The ΔE_a for the allyldifluorosilane amounts to 15.3 kcal/mol. Only one retention transition state is optimized for allyltrifluorosilane; optimizations starting from both the TS_{inv} and TS_{ret} reached the same transition structure. On the other hand, substitution of a methyl group at the equatorial position of the TS_{inv} shows no significant effects on the E_a, while the substitution at the axial positions destabilizes the TS_{inv}. The methyl substitution for TS_{ret} shows little effects on the E_a, and therefore, the methyl substitution does not affect the ΔE_a (11.7 kcal/mol).

Since aromatic groups are substituted in the allylsilanes investigated by Kwart et al.,[3] we have investigated the effects of a vinyl substituent as a typical π system. Vinyl substitution at the equatorial position in TS_{inv} (TBP) and the apical position in TS_{ret} (SP) are examined. As shown in Table 4, the E_a for the TS_{inv} is significantly lowered by the vinyl substitution (−4.0 kcal/mol), while little effects are exerted on the E_a for TS_{ret} by the substitution at the apical position (0.3 kcal/mol). Significant lowering of the ΔE_a is achieved by the vinyl substitution. These vinyl substituent effects are enhanced by incorporating electron correlation; the activation energy for TS_{ret} is 54.3 and 57.6 kcal/mol at MP2/6-31G* and MP3/6-31G* calculations, respectively, at the HF/6-31G*-optimized geometry, while those for TS_{inv} are 58.0 and 61.9 kcal/mol. In the most stable geometry, the vinyl substituent is arranged to gain the highest π conjugation with the Si 3p orbital which has the major contribution in the TS_{inv}. Substitution by phenyl and naphthyl groups at silicon in the experimental study may therefore account in part for the difference in stereochemical outcome between the 1,3-silyl migrations in a model allylsilane and the experimental allylic silanes.

Finally, the experimentally observed stereochemistry may originate from the steric effects due to bulky substituents at silicon; these substituents will elongate the distances between the silyl group and the allyl part at the transition structures. Since, as discussed above, the TS_{ret} is stabilized by subjacent orbital control through significant overlap between a silicon 3p orbital and a 2pπ orbital of the central carbon, the destabilization by bulky substituents in the TS_{ret} will be larger than that in the TS_{inv}, which may also reverse the relative stability between TS_{ret} and TS_{inv}.

Conclusion

Present calculations show that the thermal 1,3-silyl migration in allylsilane may occur via two transition states with different stereochemical configurations at silicon, where the transition state with inversion of configuration (TS_{inv}) has a trigonal bipyramidal (TBP) structure and that with retention of configuration (TS_{ret}) has a square pyramidal (SP) structure. In the TS_{ret}, the distance between the allylic central carbon and the silicon is shorter than those between the allylic terminal carbons and the silicon. Both TS_{inv} and TS_{ret} have closed-shell electronic configurations. The structure of the TS_{ret} is completely different from the transition structure for 1,2-silyl migration, which has an open-shell electronic configuration.

The activation energies (E_a values) calculated by incorporating electron correlation effects are in good agreement with the experimental activation energies. Rather unexpectedly, the E_a for the TS_{ret} is smaller than that for TS_{inv}, in contrast to the experimental situation.

Analysis of the orbital interaction in the transition states showed that the major stabilization of the TS_{inv} is caused by the MO interaction between the low-lying LUMO (θ_3) and the allyl ϕ_2 orbital, as predicted by the Woodward−Hoffmann rules, while the major stabilization in TS_{ret} is caused by a subjacent orbital control.

Substitution of either a fluorine or a methyl group at the equatorial position of TS_{inv} exerts significant effects on the activation energies, whereas the stereochemical preference as well as the difference of the E_a values do not change. On the other hand, the E_a for the TS_{inv} is lowered remarkably by introduction of a vinyl substituent at silicon. The destabilization by sterically bulky substitutents in the TS_{ret} is larger than that in the TS_{inv}, which may reverse the relative stability between TS_{ret} and TS_{inv}. Preference of inversion stereochemistry for the 1,3-silyl migration found experimentally may be caused by the electronic stabilization of the TS_{inv} by π substituents as well as the destabilization of the TS_{ret} by sterically bulky substituents.

The present theory suggests that a concerted 1,3-silyl migration with retention of configuration will be realized by the choice of appropriate substituents at silicon.

Acknowledgment. We are grateful to Professor Shinichi Yamabe, Nara University of Education, and Professor Tamás Veszprémi, Technical University of Budapest, for their valuable discussions.

Supporting Information Available: Detailed geometrical parameters of ground-state structures and transition structures for 1,3-migrations of 1-butene, allylsilane, allylgermane, and allylstannane (2 pages). See any current masthead page for ordering and Intermet access instructions.

JA9630506